Nuclear Instruments and Methods in Physics Research A 772 (2015) 63–71

Contents lists available at ScienceDirect

Nuclear Instruments and Methods in Physics Research A

journal homepage: www.elsevier.com/locate/nima

The multianalyser system of the three axes neutron spectrometer PUMA: Pilot experiments with the innovative multiplex technique

Oleg Sobolev [a], Ron Hoffmann [a], Holger Gibhardt [a], Norbert Jünke [b], Andreas Knorr [a], Volker Meyer [a], Götz Eckold [a,*]

[a] Institute for Physical Chemistry, Georg-August-University of Göttingen, Tammannstr. 6, D-37077 Göttingen, Germany
[b] Forschungs-Neutronenquelle Heinz-Maier-Leibnitz, Technical University of Munich, Lichtenbergstr. 1, D-85748 Garching, Germany

ARTICLE INFO

Article history:
Received 16 September 2014
Received in revised form
27 October 2014
Accepted 2 November 2014
Available online 11 November 2014

Keywords:
Three axes spectrometer
Multiplex techniques
Kinetics
Neutron spectroscopy
Real-time experiments

ABSTRACT

A new type of multiplex technique for three axes neutron spectrometers has been realized and successfully commissioned at the PUMA spectrometer at FRM II. Consisting of eleven analyser-detector channels which can be configured individually, this technique is especially suitable for kinetic experiments where a single excitation spectrum is recorded as a function of time without the need to move the spectrometer. On a time-scale of seconds an entire spectrum can be recorded thus allowing users to monitor changes during fast kinetic processes in single shot experiments without the need for stroboscopic techniques. Moreover, the multianalyser system provides an efficient and rapid tool for mapping excitations in ($\mathbf{Q}$,ω)-space. The results of pilot experiments demonstrate the performance of this new technique and a user-friendly software is presented which assists users during their experiments.

1. Introduction

Three axes spectrometers (TAS) are regarded as one of the most flexible and versatile instruments for inelastic neutron scattering. Invented by Brockhouse in the 50ies of the last century [1] this type of neutron spectrometer is a direct visualization of the scattering triangle defined by the incident and scattered neutron wave vectors $\boldsymbol{k_i}$ and $\boldsymbol{k_f}$ as well as the wave vector transfer $\mathbf{Q}$ to the sample. Being able to determine scattering intensities at arbitrary points in a large part of the four-dimensional ($\mathbf{Q}$,ω)-space with well-defined and adaptable resolution, a three axes spectrometer provides high quality data for the characterization of excitations in solids. As a drawback, however, it is usually restricted to a point-by-point measuring strategy which is rather time-consuming and does not allow kinetic investigations of short time scales well below some minutes unless stroboscopic techniques are employed [2]. Hence, great endeavors have been made in the past to increase the output of three axes spectrometers by using focusing optics and multiplexing techniques. Although focusing monochromators and analysers usually spoil the resolution in $\mathbf{Q}$-space [3], high resolution investigations frequently use well collimated beams where only the central part of the large monochromators or analysers available at modern spectrometers are effectively used.

Multiplex systems use arrays of analysers which are located at different scattering angles thus providing simultaneous access to multiple momentum transfers.

Flat-cone is one of the most attractive systems since it provides a constant energy analysis simultaneously for a wide range of scattering angles using an array of vertically reflecting analysers and detectors [4]. Another approach is the const. E-MARX type of analyser [5] which has been further improved in the RITA-type spectrometers [6,7]. Here, the array of analysers collects the neutrons scattered at different angles from the sample but usually with the same energy transfer and sends them towards a position sensitive detector.

We have used a still more flexible approach for the adaptation of multiplexing to the needs of specific instruments, where the restriction of constant energy is dropped and a sequence of analysers and detectors is used which provides us with the opportunity to adapt the configuration very efficiently to the type of excitation under consideration. It thus acts as three axes instrument with multiple secondary spectrometers consisting of eleven individual analysers and detectors. This innovative multi-analyser (MA) concept which is now ready for operation was included already in the first design study of the thermal three axes spectrometer PUMA at the FRM II [8] and is also responsible for part of its name. Subsequently, a similar design has been proposed for the cold TAS IN12 at the Institute Laue-Langevin [9].

* Corresponding author. Tel.: +49 551 3933143; fax: +49 551 3912592.
E-mail address: geckold@gwdg.de (G. Eckold).

http://dx.doi.org/10.1016/j.nima.2014.11.007

In this article we want to present the layout of the multianalyser-system installed at the PUMA-spectrometer in Garching, along with its different modes of operation. Moreover, the results of first test experiments are shown to demonstrate the performance of this new type of multiplex-system. Although its versatility is a great advantage on the one hand, it also poses a great challenge for the practical use, on the other hand. Therefore, we present a software system that was developed to assist the user in finding the most appropriate configuration of the multiplex system for the particular experimental problem.

2. The PUMA-multianalyser system

2.1. Design and characteristic properties

The basic design of the three axis spectrometer PUMA@FRM II is shown in Fig. 1. Neutrons from the thermal source of the FRM II reactor source are extracted through the beam tube SR7. The cross section of the beam is adapted to the needs of a particular experiment by an adjustable entrance slit located within the biological shielding. The doubly focusing monochromator (switchable between PG(002), Cu(111), Cu(220), Ge(311)) selects neutrons with a desired energy or wavelength out of the white spectrum delivered by the moderator. The monochromatic beam hits the sample which is located on a turntable to allow the accurate orientation of single crystals (ψ). For special cases, where a three dimensional variation of the orientation is needed, an Eulerian cradle can be used. The variation of the wavelength of incident neutrons is achieved by changing the monochromator angle θ_M and moving the sample table on air cushions around the monochromator. Neutrons scattered at the sample under a selected scattering angle ϕ are collected by the integrated analyser-detector system, which is moving around the sample position. Within a common shielding against background radiation, the focusing analyser selects neutrons of a particular energy from the scattered beam which are finally registered in the ^{3}He-detector. The final energy can be varied by rotating the analyser crystal (PG(002) or Ge(311)) (θ_A) and moving the detector accordingly. If required, collimators can be used for the accurate definition of the beam directions and divergencies. Most of the components of the spectrometers including monochromators and collimators can be changed automatically allowing for a user-friendly mode of operation. By varying the four main axes of PUMA, that is, monochromator angle θ_M, sample orientation ψ, scattering angle ϕ and analyser angle θ_A, almost arbitrary combinations of momentum-($\hbar\mathbf{Q}$)-and energy-($\hbar\omega$)-transfer from the neutron to the sample can be selected and the scattered intensity determined.

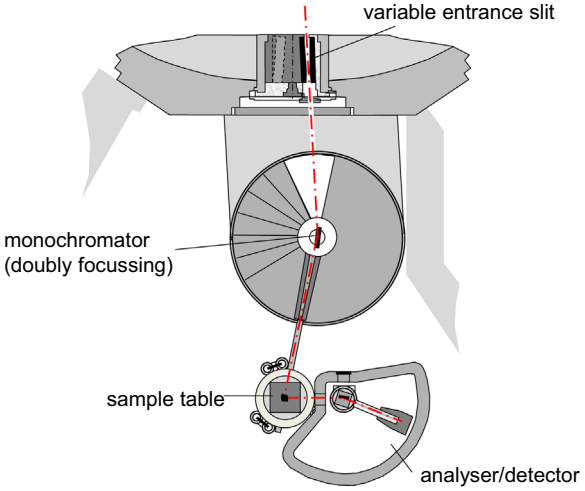

Fig. 1. Layout of the three axis spectrometer PUMA in its basic version.

On top of this basic layout, a multiplex system was installed at PUMA which consists of an array of eleven individual analyser crystals and eleven individual detectors as shown schematically in Fig. 2. This system covers a range of scattering angles of up to 16° and allows the detection of neutrons with different energies.

The (vertically focusing) PG(002)-analysers are blades of 25 mm width and 150 mm height which are mounted on individual turn tables and rails allowing rotation and translation along the beam. The detectors are conventional 1"-tubes filled with 10 bar ^{3}He moving individually around the center of the analyser module over an angular range of about 140°. In order to avoid crosstalk between different analyser-detector channels, each detector is equipped with a guide with Cd-coated walls that can be rotated to point exactly to the associated analyser crystal, as shown schematically on the left hand side of Fig. 2. The width of these guides is automatically adapted to the effective width of the corresponding analyser. A photograph of the actual set-up is shown in Fig. 3.

Hence, each of the individual analyser-detector channels can be configured rather arbitrarily in order to select neutrons of different energies.

The whole system consists of 44 stepper motor drives (rotation and translation of analysers and detectors) with accuracies better than 0.01° or 0.1 mm. The control electronic is highly integrated using modules for six individual axes (including the stepper motor endphases) on one single euroboard.

Although the system of eleven single detectors is most appropriate for the divergent configuration shown in Fig. 2, a convergent

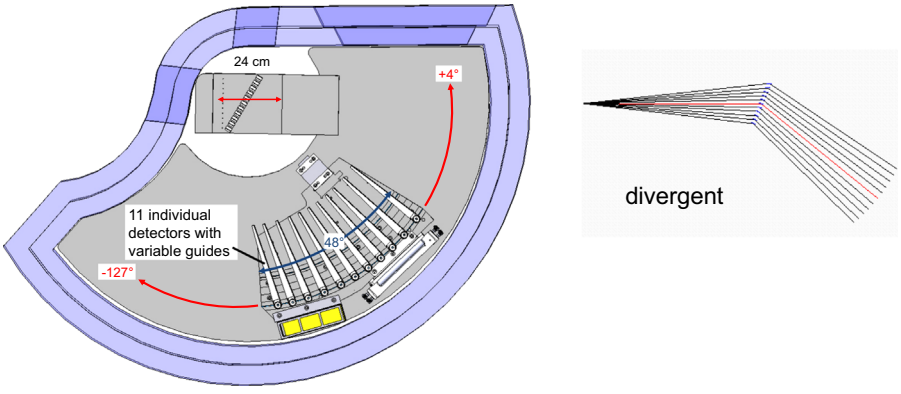

Fig. 2. Design of the multianalyser system consisting of 11 analyser crystals and 11 individual detectors with variable beam guides. This version is suited for divergent configurations as illustrated on the right hand side.

situation as depicted in Fig. 4 might also be useful for certain applications. Here, the analyser crystals are arranged in a way to focus all reflected neutrons onto a point between analyser and detector. An adjustable slit (0–30 mm width) at this position helps to reduce background and crosstalk, but the spatial separation of the individual channels at the detector remains rather small and prevents the use of single detector tubes. Hence, seven horizontal position sensitive detector tubes are installed which cover the full beam height and which can be moved as a whole around the analyser centre. Fig. 5 shows a photograph of this arrangement.

It should be added that the distance between sample and analyser can be varied continuously and the entire arrangement of the rails for the individual analysers can be rotated with respect to the central beam. Both features may be used to vary the separation of the individual beam channels and their efficient collimation which is determined by the geometrical parameters.

In order to meet the requirements for accurate and reproducible experiments, the sophisticated and extremely compact design needs very careful manufacture and adjustment processes. It was shown in numerous tests during commissioning that both, the high-precision mechanical devices and the electronic control systems developed at the University of Goettingen in fact allow the reliable operation of this demanding system.

2.2. Theory of operation

The PUMA multianalyser system allows the simultaneous detection of scattering intensities at eleven different positions in $(\mathbf{Q},\omega)$-space. Hence, a suitable configuration can provide an entire scan across an excitation of the sample under consideration.

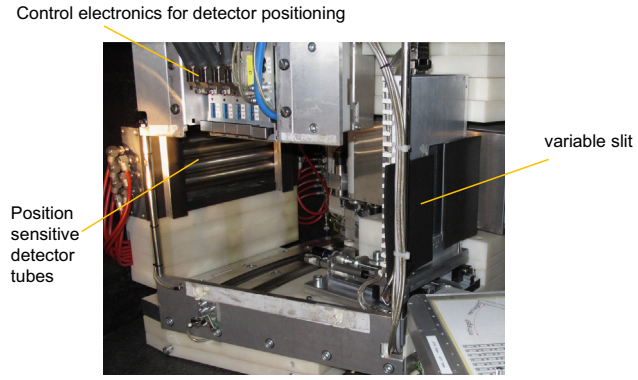

Fig. 5. View of the horizontal PSD-tubes and the variable slit for convergent configurations.

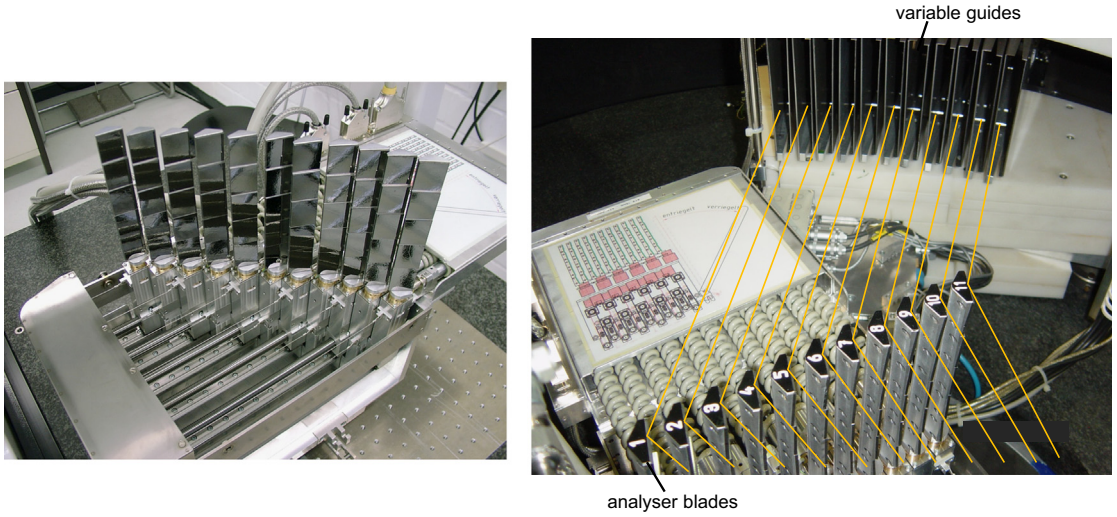

Fig. 3. Left: Arrangement of 11 individual analyser blades which can individually be rotated and translated. Right: View of the analyser-detector system. The neutron paths for the 11 individual channels are indicated as coloured lines.

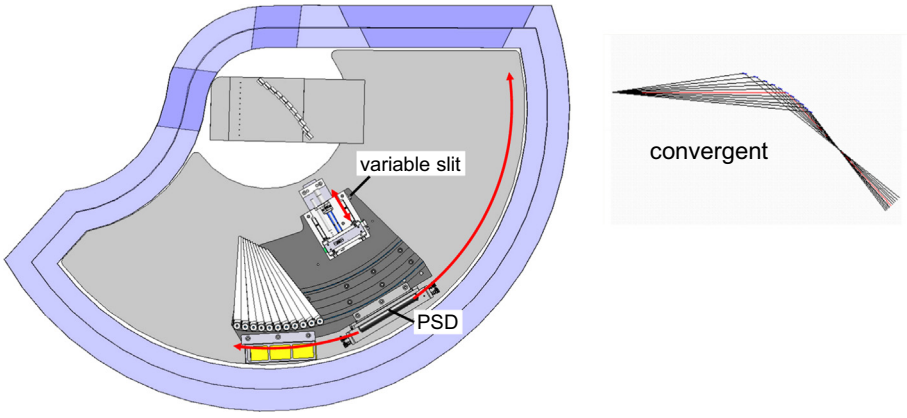

Fig. 4. Convergent configuration using position sensitive detectors (PSD) and a variable slit for background reduction.

Obviously, each analyser receives neutrons scattered at a different angle. Hence, a const. **Q**-scan cannot be realized. But for most experiments this is not really needed as will be shown below. The accessible range in **Q**-space can be visualized most directly in the representation of scattering triangles as shown in Fig. 6. The nominal setting of the spectrometer, that is, the channel corresponding to the central analyser crystal, is given by the scattering vector $\boldsymbol{Q}_o$ and the wave vectors of incident and scattered neutrons $\boldsymbol{k}_i$, and $\boldsymbol{k}_f^o$, respectively, ϕ being the scattering angle between both vectors. Any of the other multianalyser channels corresponds to a different scattering angle $\phi + \Delta\phi$ and, hence, to a different direction of the final wave vector $\boldsymbol{k}_f$. The analyser angle chosen for this particular channel determines the length of $\boldsymbol{k}_f$ and, consequently, the energy transfer $\hbar\omega$. From Fig. 6, it is readily seen that this leads to a variation $\boldsymbol{\Delta Q}$ of the scattering vector with components parallel and/or perpendicular to $\boldsymbol{Q}_o$.

Unlike a normal TAS with a focusing analyser crystal which collects monochromatic neutrons scattered into a large solid angle, the multianalyser system is almost equivalent to eleven individual secondary spectrometers. Each of these individual channels is operating with a well-defined divergency since the effective collimation is essentially given by the size of the analyser blades and the distance between sample and analyser. For $k_f = 2.662$ Å^{-1}, for example, the effective collimation is about 30' (using a sample-analyser distance of 1000 mm and PG(002)-reflection) and decreases to about 20' for $k_f = 4.1$ Å^{-1}.

As a special setting, however, the multianalyser can also be used as a conventional focussing analyser when all blades are oriented to reflect neutrons of the same energy. With a total width of 11×25 mm $= 275$ mm, its acceptance angle is larger than that of the standard PG-analyser which leads to an overall increase of the total intensity. But as the main advantage, the multianalyser system records the signal from different analyser crystals separately, which can be very useful for background subtraction and discrimination of the spurious signals. Moreover, taking into account the above mentioned effective collimation for the individual analyser blades, the user can decide afterwards whether it is useful to sum up the signal from all analysers or to use only central channels.

2.3. Modes of operation

The flexible multianalyser system allows a great variety of different scans, both, for convergent or divergent configurations. Among them there some special cases:

- *Scans along well defined directions in* **Q***-space* The analyser angles are chosen to provide a path corresponding to continuous variation of the scattering vector along a direction which makes an angle ζ with respect to the nominal momentum transfer $\boldsymbol{Q}_o$ as illustrated in Fig. 7.
  $\zeta = 0$ is a special case, where **Q** varies along the nominal direction of $\boldsymbol{Q}_o$ while $\zeta = 90^\circ$ corresponds to the perpendicular direction which is particularly interesting for the investigation of transverse phonons, for example,
- *Scans with a well-defined energy range* The analyser angles are chosen to cover a suitable energy range in equal increments. The scattering vectors will vary accordingly. A constant-energy scan is a special case.
- *Scans with constant modulus of* **Q** In this case, the end-points of $\boldsymbol{k_f}$ are located on a circle around the end-point of $\boldsymbol{Q_o}$.

The position of the different analysers along their rails can also be chosen quite arbitrarily and determines essentially the separation of the individual beam paths towards the detector. Hence, geometrical constraints due to the mechanical arrangement of analysers and detectors within the common shielding can be overcome by a careful selection of the analyser positions. For each of the blades, the analyser angle can be varied continuously up to 50° which corresponds to a minimum value $k_f^{min} = 1.22$ Å^{-1} if the PG(002) reflection is used. Only if the lateral separation of two neighbouring blades is too small (less than about 1 cm) the accessible angular range is somewhat reduced.

2.4. Software-support

Since the PUMA multianalyser system is extremely flexible and versatile, its efficient use requires a user-friendly computer software for the detection of suitable configurations and measuring strategies for a particular experimental problem since the user cannot be expected to know about the details of different modes of operation. Hence, we have developed a self-optimizing software system MAX-1 which assists the user during his experiments and finds automatically a selection of the most appropriate configurations.

It is assumed that the user has some idea about the dispersion of the excitation to be detected. The specification of the dispersion surface and the scan center allows the optimization of the multianalyser-scan. For different incident neutron energies, the program MAX-1 checks all possible configurations (for converging or diverging modes) and determines some figures of merit (FOM) which are subsequently used to select the most appropriate setting of the multianalyser. One FOM is defined by the angle between the scan direction and the normal to the dispersion surface which should be small. Another FOM is the scan range with respect to the resolution which is calculated according to [3]. Other types of FOM may be added. For each of the possible configurations, MAX-1 provides the illustration of the scan paths both, in direct and reciprocal space. Moreover, it simulates the expected intensity profile. In Fig. 8, examples for typical output data of MAX-1 are presented.

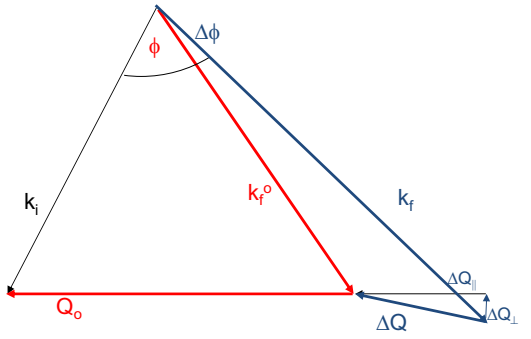

Fig. 6. Scattering triangle for the central (nominal) channel (red) and another selected channel of the multianalyser system (blue).

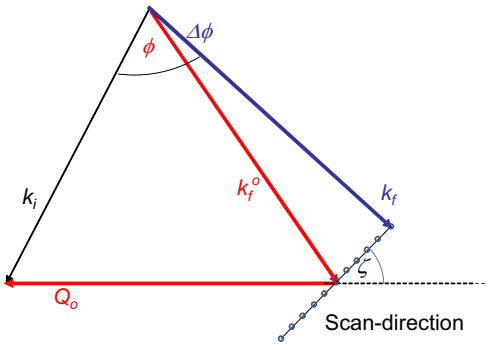

Fig. 7. ζ-scan where the wave vectors of scattered neutrons end on a line which is inclined with respect to nominal Q_o by the angle ζ.

Moreover, the program also analyses possible higher order contamination effects and issues a warning if spurious intensity might be expected due to elastic scattering. It also optimizes the positioning sequence of all 44 axes of the multianalyser and multidetector in order to save positioning time.

3. Results from pilot experiments for the demonstration of the multianalyser performance

3.1. Acoustic phonons in germanium

In order to demonstrate the performance of the multianalyser-system, we have performed a number of experiments on model systems. As an example, the profile of an acoustic phonon of germanium is shown in Fig. 9 for a scan across the TA-dispersion surface as obtained using the divergent mode at k_i=3.8 Å^{-1}. The total counting time was 1 s for the entire spectrum for a scattering volume of the sample of several cm^3. Even if the scan is not taken at constant **Q**, the phonon is well defined. The signal-to-background ratio ($\sim$ 60) is at least comparable to what is observed in normal three-axes mode thus proving the efficiency of the detector guide system. Similar scans of optical (Γ-point) phonons with frequencies near 9 THz need a total counting time of 2 min in order to achieve similar count rates.

The resolution is well described by the theoretical formalism described in [3] and corresponds to standard TAS mode if one considers the effective collimation of about 30' as given by the geometrical parameters.

Obviously, the multianalyser system allows the detection of phonons on an unprecedented time-scale of seconds or minutes which indeed opens new prospects for time-resolved studies which appear to become more and more important for future applications of neutron scattering [10].

3.2. Softmodes in quartz

As a pilot experiment for kinetic investigations, we have studied phonons in quartz during a rapid temperature variation. The well-known phase transition at about 573 °C is associated with the softening of optical phonons both, at center and at the boundary of the Brillouin zone. Moreover, due to anticrossing effects even the acoustic phonons are affected and exhibit significant temperature variations as demonstrated in the extensive work of Axe et al. [11], Boysen et al. [12], Berge et al. [13], or Gibhardt [14].

Fig. 10 shows the measured phonon dispersion of quartz at room temperature [15] along with the proposed and estimated variation of two optical modes on heating towards the phase transition [12]. Both optical modes near 4 THz (in the following referred to as A-mode) and 6 THz (B-mode) are rather flat at room temperature but exhibit a strong dispersion near the phase transition. The frequency of the B-mode is assumed to remain fixed at the zone boundary (M-point) and decreases to less than 1 THz at the Brillouin zone center thus driving that phase transition. The A-mode, however, exhibits the opposite behaviour, being stable at the Γ-point but softens at the M-point.

There are only few experimental data on the softening behaviour [11,12,14] in the low-temperature phase which may be due to the strong damping effects which makes the observation difficult. The PUMA-multianalyser system is a versatile tool to study this complicated behaviour as will be shown in the following.

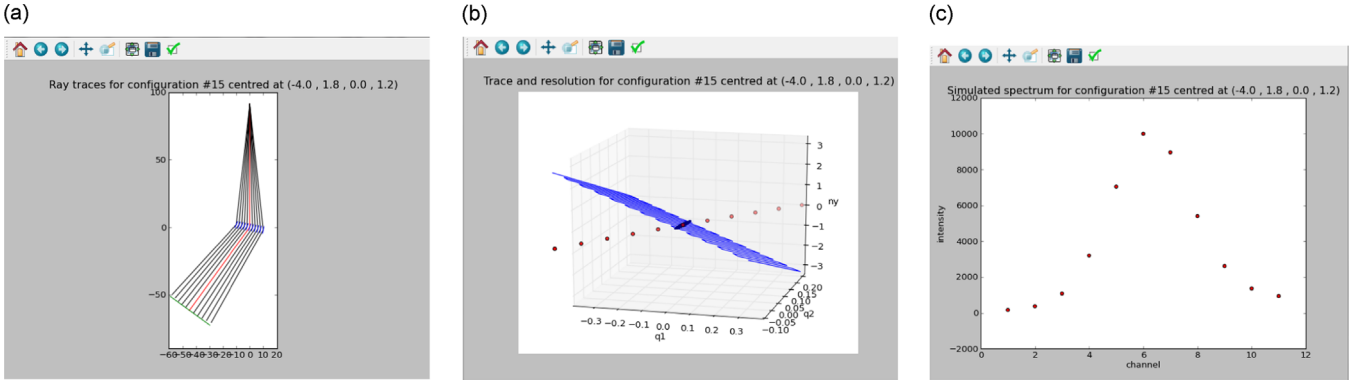

Fig. 8. Some impressions of the self-optimizing program MAX-1: a) View of analyser channels in direct space for a selected configuration b) Trace of scan points in (**Q**,ω)-space along with the dispersion plane and the resolution ellipsoidc) Simulated spectrum.

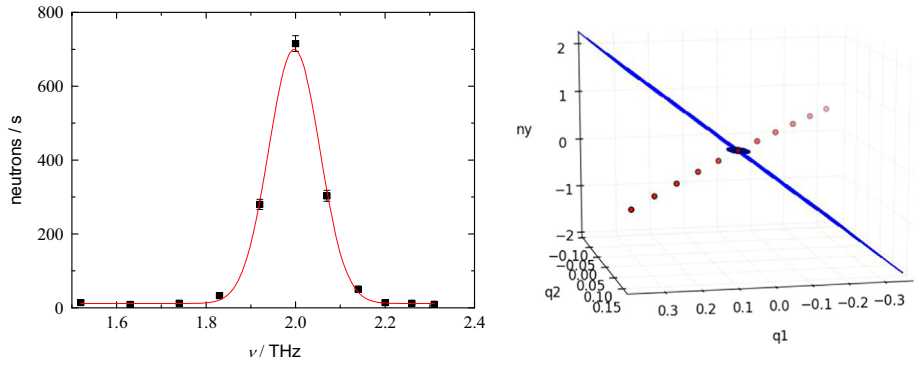

Fig. 9. TA phonon of Germanium at **Q**=(4 0.4 0) detected in 1 s total counting time. The trace of scan points in (**Q**-ω)-space is illustrated on the right hand side along with the dispersion surface and the resolution ellipsoid for the central channel.

The quartz single crystalline sample used for our experiments was cut from a large industrial grown crystal and had a size of about $5 \times 5 \times 6$ mm³. It was oriented with the trigonal axis perpendicular to the scattering plane. For demonstration purposes, we selected multianalyser-scan at constant energy $\nu = 1.2$ THz across the transverse acoustic mode within the symmetry plane. The trace in $\boldsymbol{Q}$-space is indicated on the left hand side of Fig. 11. During cooling and heating between 100 and 550 °C with temperature rates of about 4 K/min we took spectra every 5 min. The results are displayed on the right hand side of Fig. 11 where the scattered intensity is shown in a contour plot as a function of scan-variable (analyser-channel, h and k) and time (temperature). The scattered intensity becomes much larger at high temperatures due to the Bose-occupation factor. But there is also a shift of the phonon center to larger wave vectors when approaching the transition temperature of 573 °C corresponding to a softening of the acoustic branch. This is due to the interaction with the optical A-mode which belongs to the same irreducible representation. This effect starts already at low temperatures but becomes more and more pronounced until the maximum temperature of this cycle is reached at 550 °C.

When comparing the behaviour during heating and cooling one easily recognizes that the results are perfectly reproducible. The total counting time of 5 min per time-step is clearly sufficient to provide enough counting statistics even at low temperatures. The whole sequence during cooling and heating took about 5 h.

Similarly, we studied the temperature dependence of the optical phonons directly. A scan centered at the Γ-point (−4 2 0) and 3 THz with a wide frequency spread of about 4 THz was selected to monitor the behaviour of the lowest optical branch. In Fig. 12 the results for a temperature interval between 100 °C and 550 °C are shown along with the trace of the scan in $\boldsymbol{Q}$-ν-space. The broad frequency interval is associated with the variation of scattering vectors across the entire Brillouin-zone in a direction which is close to (1–1 0). At very small frequencies, the residues of the diffuse elastic scattering are recognized which become more and more important at higher temperatures. This is most pronounced in channel 1 (which is omitted in this Figure) and can still be seen in channel 2 at higher temperatures.

There is a very broad and continuously decreasing intensity distribution in channels 3 to 8, that is, up to frequencies of about 4 THz, that is due to the optical branch A and acoustic modes which contribute for scattering vectors different from the zone center. On approaching the phase transition temperature, however, the optic mode dominates and a broad maximum is observed in channel 5 corresponding to the wave vector $\boldsymbol{Q}=(-4.11, 2.09, 0)$ and frequency $\nu = 2.52$ THz. This finding corresponds quite well to the suggestions of Boysen et al. [12] for the soft mode behaviour.

Another interesting result is obtained at higher energies where the temperature dependence of the true softmode B is observed. In Fig. 13, the results for a scan in the frequency range between 4 and 6 THz are shown along with its trajectory across the phonon dispersion curves. Here, a scan was chosen with scattering vectors along the longitudinal (100)-direction.

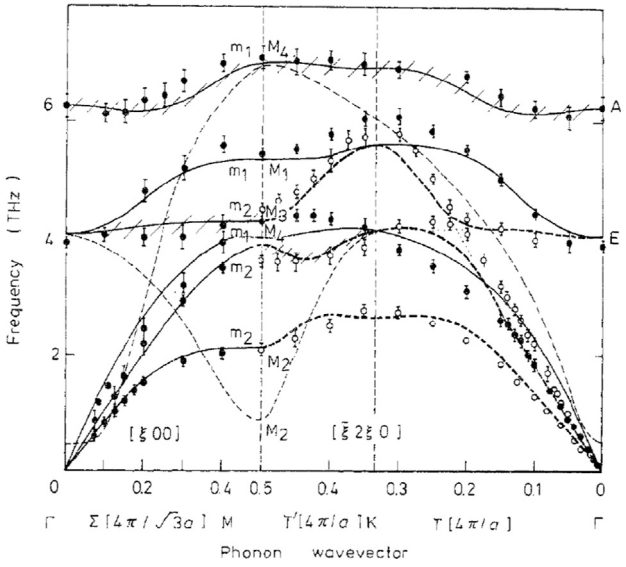

Fig. 10. Phonon dispersion of quartz at room temperature as determined by Dorner et al. [15]. The estimated softening of two optic branches near 4 THz and 6 THz (illustrated by hatching) is indicated by dashed lines [12].

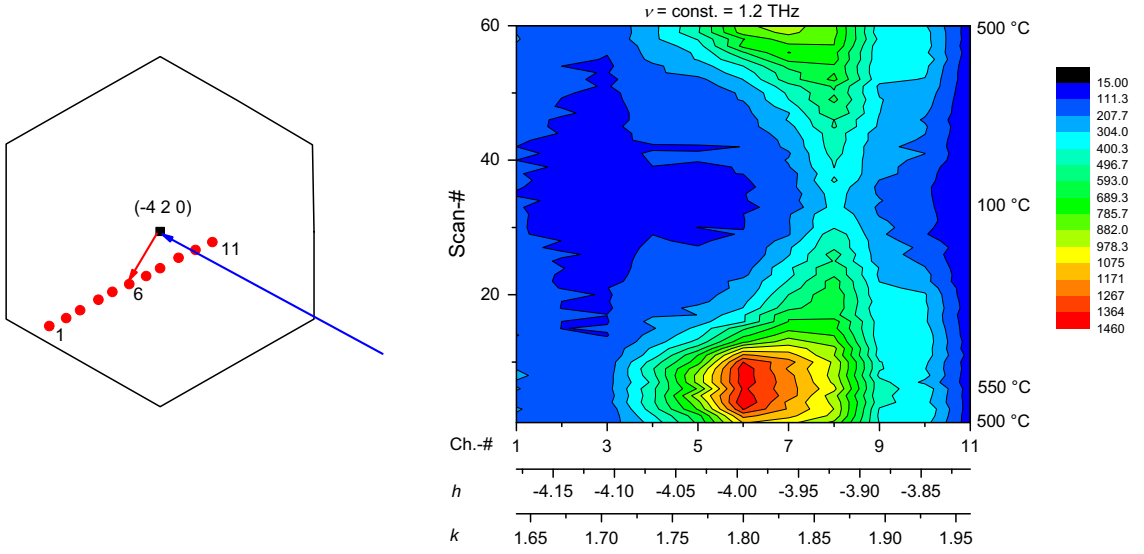

Fig. 11. Temperature dependence of a constant energy scan across the transverse acoustic phonon of quartz: left: trace of a multianalyser scan within the Brillouin-zone (-4 2 0) (red dots). The arrows illustrate the direction of the reciprocal lattice vector (blue) and the phonon wave vector at the center of the scan (red), respectively. right: contour map of the time-evolution of the scattered intensity as obtained within 5 minutes counting intervals during cooling and heating. The incident neutron energy was selected to be $k_i = 3.6$ Å^{-1} and the total data-acquisition time was 5 hours.

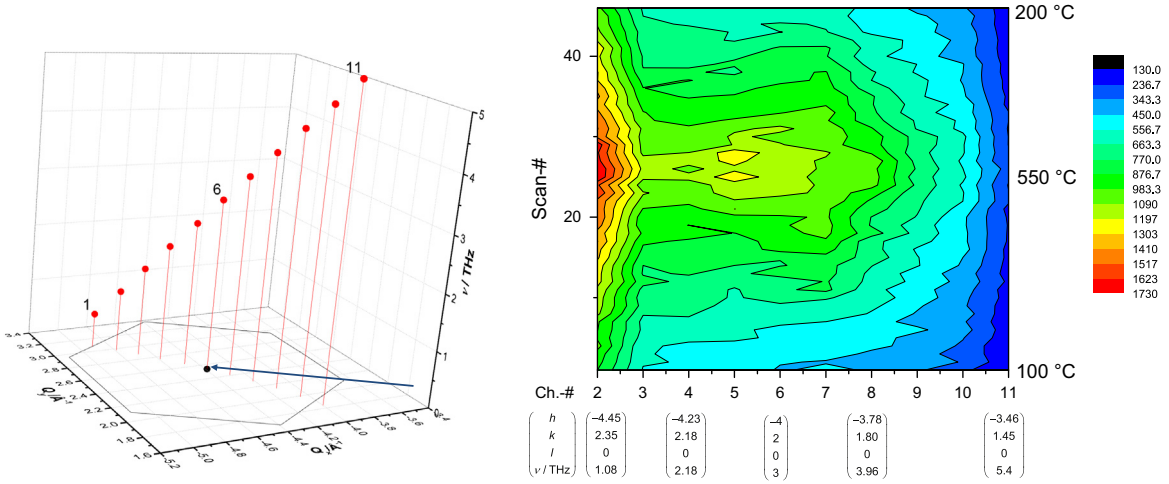

Fig. 12. Temperature dependence of a scan across the low frequency optical phonon branch A of quartz: left: trace of a multianalyser scan within the Brillouin-zone (-4 2 0) (red dots). The blue arrow illustrates the direction of the reciprocal lattice vector at the center of the scan. right: contour map of the time-evolution of the scattered intensity as obtained within 5 minutes counting intervals during cooling and heating. The incident neutron energy was selected to be k_i=4.6 Å^{-1} and the total data-acquisition took about 4 hours.

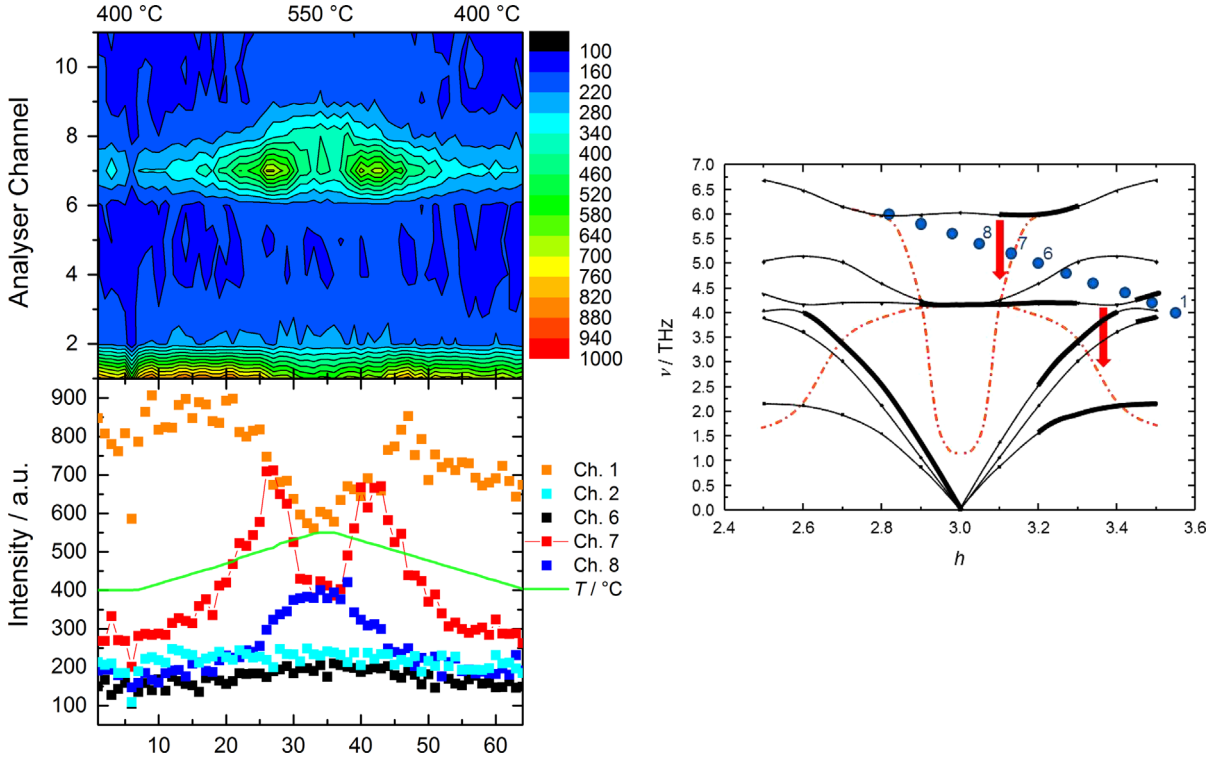

Fig. 13. Temperature dependence of a scan across the high frequency optical phonon branch B of quartz with a longitudinal variation of **Q**: right: trace of a multianalyser scan within the Brillouin-zone (3 0 0) (blue dots) along with the phonon dispersion in direction (100). The dotted lines are results of model calculations at room temperature and the highlighted bold parts indicate the ranges within the (300)-Brillouin zone with large structure factors. left: contour map of the time-evolution of the scattered intensity as obtained within 5 minutes counting intervals during cooling and heating. The incident neutron energy was selected to be k_i=4.4 Å^{-1}. The intensity profiles for selected analyser channels are also shown along with the corresponding temperature profile.

At elevated temperatures, a pronounced intensity maximum in channels 7 and 8 is observed close to the zone center near 5.5 THz. This corresponds to the softmode B which exhibits a well-defined maximum of its structure factor near (3.15 0 0) as confirmed by model calculations using the program package UNISOFT [16]. Interestingly, this maximum is smeared out at the highest temperature of about 550 °C, reflecting directly the anharmonic behaviour of the Γ-point softmode. Moreover, the data also prove that the softening is confined to small phonon wave vectors since in channel 6 which corresponds to a wave vector of (3.2 0 0) the intensity is already drastically reduced and almost no temperature dependence is observed.

Channel 1, on the other hand, monitors the optical A-mode at the zone boundary as confirmed by structure factor calculations. The temperature profile in the lower part of Fig. 13 shows that the intensity is considerably reduced at high temperatures which is a clear signature of the softening of this branch at the M-point of the Brillouin zone.

Hence, the present pilot experiment is not only a proof of principle for the multianalyser system but yields at the same time

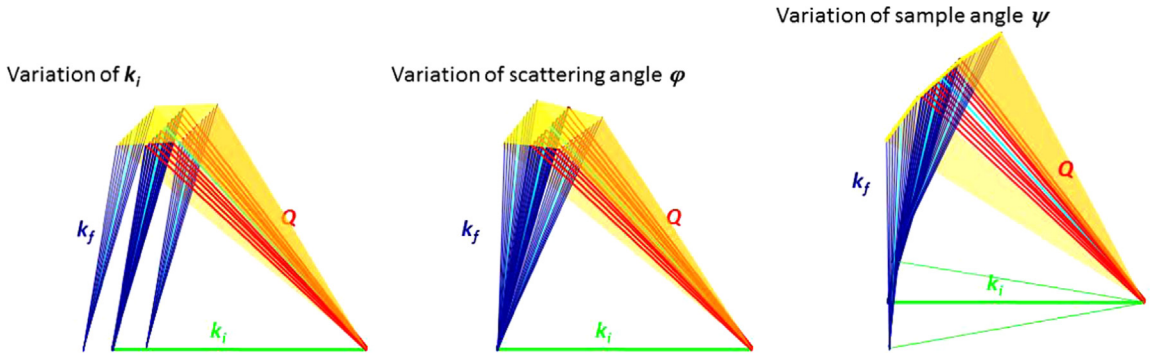

Fig. 14. Schematical illustration of the variation of incident neutron energy or k_i (left), the scattering angle ϕ (middle) and the sample orientation ψ (right) and the corresponding effect on the scattering triangle and the area which is covered by the multianalyser system.

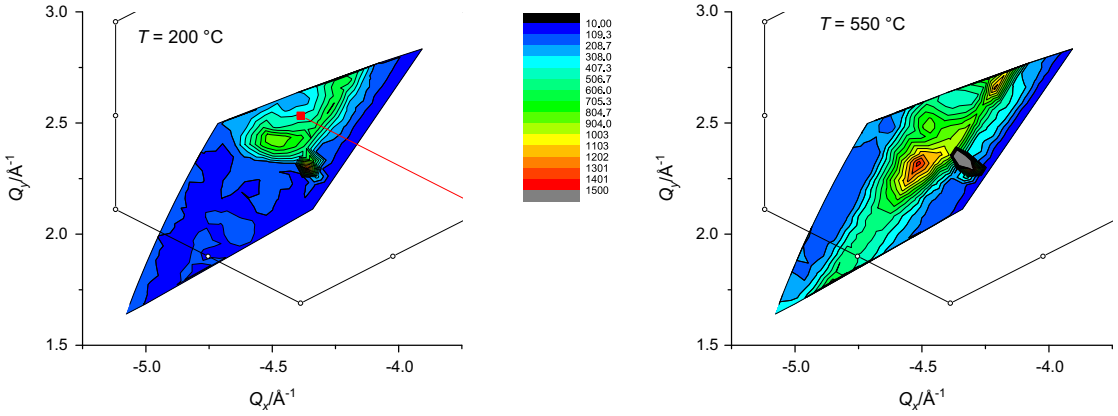

Fig. 15. Constant energy maps of phonon intensities in the Brillouin-zone (-4 2 0) for two different temperatures as obtained by multianalyser scans according to Fig. 11 and the variation of the sample angle ψ. The red line indicates the direction from the zone center towards the origin of the reciprocal lattice. Each map requires a total of 2 hours counting time.

new experimental evidence for the anharmonic behaviour of quartz which could be obtained in a very efficient way in a time-dependent mode of data acquisition.

3.3. Mapping strategies

Although the most obvious application of the PUMA-multianalyser is for real-time studies, also the mapping of excitations can be realized rather efficiently: Once a scan is prepared, a contour map can be produced by varying one of the other main axes of the spectrometer without changing the analyser. During the ψ-mapping the sample orientation is varied which can usually be realized very rapidly. Similarly, ϕ- and k_i-mappings are obtained by changing the scattering angle and the incident neutron energy (monochromator angle), respectively. Each of these mapping strategies covers a wide range of ($\mathbf{Q}$-ω)-space as illustrated in Fig. 14. Here, the scattering triangles for the individual analyser channels are shown and their variations when k_i, ϕ or ψ is altered. The different multianalyser-mapping strategies can be used to obtain an overview about excitations in solids.

For the demonstration of the performance, we used again quartz as a model system and studied the temperature dependence of softmodes and acoustic modes in a wide area of the Brillouin zone.

In Fig. 11 we have already shown the temperature variation of a multianalyser scan across the transverse acoustic branch at constant energy. If we use the same configuration and vary the sample angle ψ, we obtain a map of the phonon dispersion within the symmetry plane. This is shown for two different temperatures in Fig. 15. Although the transverse mode is reflected by an almost isotropic intensity distribution at low temperatures a very pronounced streak is observed towards the transverse M-point where the softening of the acoustic branch is expected due to its interaction with the optic A-branch according to [12] (c.f. Fig. 10). These data provide a nice overview about the temperature dependent dynamic behaviour of this fascinating compound. This representation is similar to what can be observed also by flat-cone techniques [4]. Due to the well-defined collimation of the neutron beam for the individual analyser channels, however, the present technique seems to provide a better resolution.

Moreover, the mapping strategies can now be combined with true inelastic multianalyser scans which open new opportunities for fast experiments to obtain cross sections through excitation surfaces. Even if our quartz sample had a volume of about 0.1 cm^3 only, the maps shown in Fig. 15 were obtained within 2 h each (i.e. 2 min per ψ-step).

4. Conclusion and outlook

The new multianalyser system at the three axes spectrometer PUMA@FRM II was commissioned and is now ready for user operation. It consists of an 11-fold secondary spectrometer which can be configured rather arbitrarily in order to perform general scans in ($\mathbf{Q}$-ω)-space. Due to its sophisticated design, the PUMA-multiplex system combines all the advantages of usual three axes instruments with the ability to measure different scan points simultaneously. In particular, the very efficient background

reduction and the effective collimation allow very accurate and selective experiments.

It could be shown that all of the demanding requirements for this compact multiplex technique could be achieved. Moreover, a user-friendly software system was developed that allows the efficient use of this new and versatile instrument.

In pilot experiments using germanium and quartz single crystals it could be demonstrated that single phonon spectra can be obtained on a time scale of seconds. This opens new possibilities for kinetic studies since it allows the in-situ determination of changes of interatomic interactions and chemical bonds during solid state processes such as reactions, phase transitions or during external loads. The softmode behaviour in quartz could be studied in some detail providing new details about the anharmonic features which were hitherto not proven experimentally.

Acknowledgement

This work is funded by the German Federal Ministry for Education and Research (BMBF) under contract no. 05K10MG2

References

[1] B.N. Brockhouse, Inelastic Scattering of Neutrons in Solids and Liquids, Proc. IAEA Symp. (1961) 113.
[2] G. Eckold, Nucl. Instrum. Method A 289 (1990) 221;
G. Eckold, in: G. Eckold, H. Schober, S.E. Nagler (Eds.), Studying Kinetics with Neutrons, 161, Springer Series in Solid State Sciences, 2010, pp. 177–211.
[3] G. Eckold, O. Sobolev, Nucl. Instrum. Method A 752 (2014) 54.
[4] J. Kulda, Nucl. Eng. Technol 38 (2005) 433.
[5] R. Scherm, V. Wagner, Neutron Inelastic Scattering, IAEA (1977) 149 (in).
[6] K. Lefmann, Physica B 283 (2000) 343.
[7] F. Demmel, et al., Nucl. Instr. Meth. A 530 (2000) 404.
[8] P. Link, G. Eckold, J. Neuhaus, Physica B 276-278 (2000) 122.
[9] W. Schmidt, M. Ohl, Physica B 385-386 (2006) 1073.
[10] (see e.g), G. Eckold, H. Schober, S.E. Nagler (Eds.), Studying Kinetics with Neutrons, 161, Springer Series in Solid State Sciences, 2010, pp. 177–211.
[11] J.D. Axe, G. Shirane, Phys.Rev. B 1 (1970) 342.
[12] H. Boysen, et al., J. Phys. C: Solid State Phys 13 (1980) 6127.
[13] B. Berge, et al., Ferroelectrics 66 (1986) 73.
[14] H. Gibhardt, (Thesis), University of Göttingen, 1998.
[15] B. Dorner, et al., J. Phys. C: Solid State Phys 13 (1980) 6607.
[16] G. Eckold, JÜL-2639, Jülich 1992, ISSN 0366-0885. ⟨http://www.uni-pc.gwdg.de/eckold/unisoft.html⟩.